SciMedCentral

Annals of Clinical & Experimental Metabolism

Research Article

Metformin Attenuates Expression of Endothelial Cell Adhesion Molecules and Formation of Atherosclerotic Plaques via Autophagy Induction

Cédéric F. Michiels[1], Sandra Apers[2], Guido RY De Meyer[1], and Wim Martinet[1]*

[1]*Laboratory of Physiopharmacology, University of Antwerp, Belgium*
[2]*Natural Products & Food Research and Analysis (NatuRA), University of Antwerp, Belgium*

***Corresponding author**
Wim Martinet, Laboratory of Physio pharmacology, University of Antwerp, Universiteitsplein 1, B-2610 Antwerp, Belgium, Tel: 32-3-265-26-79; Fax: 32-3-265-25-67; Email: wim.martinet@uantwerpen.be

Submitted: 23 May 2016

Accepted: 04 June 2016

Published: 06 June 2016

Keywords
- Metformin
- Atherosclerosis
- Cell adhesion
- Autophagy

Abstract

The biguanide metformin belongs to the cornerstone therapeutics in treating type II diabetes mellitus. Chronic treatment of diabetic patients with metformin also reduces the development of micro- and macrovascular complications including atherosclerosis. However, the mechanisms driving its anti-atherogenic properties, beyond those of its anti-hyperglycemic effects, are not completely understood. In the present study, we aimed to further clarify the protective effects of metformin against atherosclerosis in a non-diabetic condition. To this end, apolipoprotein E deficient (*ApoE*$^{-/-}$) mice were fed a Western-type diet for 20 weeks to induce plaque formation. Meanwhile, animals were treated with metformin (250 mg/kg/day in drinking water) or plain drinking water. Histochemical analysis of plaques in the brachiocephalic artery revealed that metformin inhibited atherosclerotic plaque development (plaque size: 236 ± 30% vs. 176 ± 18%, $P < 0.05$). Moreover, metformin-treated plaques showed a reduced amount of plaque macrophages (2.1 ± 0.3% vs. 1.3 ± 0.2%, $P < 0.05$), an increased amount of vascular smooth muscle cells (2.7 ± 0.3% vs. 3.9 ± 0.4%, $P < 0.05$) and higher collagen content (22 ± 3% vs. 33 ± 4%, $P < 0.05$). Using GFP-LC3 transgenic mice, we could demonstrate induction of autophagy by metformin *in vivo*. *In vitro* experiments with human umbilical vein endothelial cells (HUVECs) indicated that metformin down regulated the cell adhesion molecules ICAM-1 and VCAM-1, and prevented monocyte-to-endothelial cell adhesion. These effects were not evident in metformin-treated HUVECs after silencing of the essential autophagy gene *Atg7*, suggesting that metformin mediates its effects through induction of autophagy. Overall, we conclude that metformin attenuates atherogenesis and leads to a more stable plaque phenotype in non-diabetic subjects.

ABBREVIATIONS

AMPK: AMP-Activated Protein Kinase; ApoE: Apolipoprotein E; EC: Endothelial Cell; HBSS: Hank's Balanced Salt Solution; HUVEC: Human Umbilical Vein Endothelial Cell; ICAM-1: Inter Cellular Adhesion Molecule 1; mTOR: Mammalian Target of Rapamycin; NF-κB: Nuclear Factor-κB; NO: Nitric Oxide; PDGF: Platelet-Derived Growth Factor; VCAM-1: Vascular Adhesion Molecule 1; VSMC: Vascular Smooth Muscle Cell

INTRODUCTION

Atherosclerosis is a chronic inflammatory disease of the arterial vessel wall characterized by the development and progression of atherosclerotic plaques, particularly in regions with low/disturbed blood flow [1]. Advanced atherosclerotic lesions can completely occlude the blood lumen and even rupture, potentially leading to lethal cardiovascular events. Although lipid-lowering drugs such as statins are an established value in the treatment of atherosclerosis, effective prevention of atherosclerosis and its complications remains challenging [2]. Of note, the incidence of atherosclerosis is 2 to 3 times higher in diabetic patients and is magnified by existing co-morbidities [3,4]. Indeed, a growing body of evidence suggests that vascular diabetic complications are closely related to chronic inflammation and can be reduced by glucose-lowering agents such as biguanides [5,6]. The biguanide metformin has been used extensively as first-line medication during the past decades in the management of non-insulin dependent diabetes mellitus and is considered as one of the safest drugs in its class, with exceptional occurrence of lactic acidosis even in nondiabetic patients and at advanced age [7-10]. It is generally known that micro- and macrovascular complications including atherosclerosis are significantly reduced in diabetic patients after chronic metformin treatment [11-13]. However, the mechanisms of action, beyond those of its anti-hyperglycemic effects, are not fully understood [14]. Numerous reports revealed that metformin can attenuate pro-inflammatory

responses in various cell types including endothelial cells (ECs), macrophages and vascular smooth muscle cells (VSMCs) [15-17]. Metformin also appears to inhibit monocyte adhesion to ECs as well as differentiation of human monocytes into macrophages and foam cell formation [18]. Apart from vascular inflammation, a number of biochemical and mechanical factors converge on the endothelium during the development of diabetes, resulting in endothelial dysfunction with a marked decrease in nitric oxide (NO) bioavailability [19]. Metformin enhances endothelial function in human umbilical vein endothelial cells (HUVECs) by stimulating nitric oxide production, probably through up regulation of the endothelial NO synthase [20,21]. Moreover, apolipoprotein E deficient (*ApoE*$^{-/-}$) mice, fed a high-fat diet and treated with metformin, showed significantly reduced plaque formation in the thoracic aorta, an effect that was assigned to decreased senescence [14]. Finally, it is noteworthy that metformin decreases the mean platelet mass in the circulation [22] and indirectly activates AMP-activated protein kinase (AMPK) by increasing the AMP/ATP ratio via mild and transient inhibition of the mitochondrial respiratory-chain complex-1 [23]. Activated AMPK switches cells from an anabolic to a catabolic state, resulting in reduced glucose, lipid, and protein synthesis while promoting the oxidation of fatty acids and glucose uptake, which has been associated with weight loss as well as lower total cholesterol and triglyceride levels [24]. Activation of AMPK also leads to the inhibition of the mammalian target of rapamycin (mTOR). Inhibition of mTOR stimulates autophagy, which is an evolutionary preserved subcellular process that protects the cell from the accumulation of damaged cytosolic material, such as misfolded proteins and damaged organelles [25]. Recent evidence suggests that controlled induction of autophagy contributes to stabilization of atherosclerotic plaques [26-28] and that autophagy dysfunction can result in plaque progression [29-31].

Given the aforementioned anti-atherogenic effects as well as the favorable clinical safety profile and low cost, metformin has an added value as adjuvant therapy in the therapeutic strategies to control atherosclerosis in non-diabetic patients. In the present study, we aimed to further clarify metformin's underlying mechanisms driving its protective effects against atherosclerosis in a non-diabetic condition. Our data indicate that inhibition of monocyte adhesion to ECs by metformin depends on autophagy induction.

MATERIALS AND METHODS

Mice

Twenty four male *ApoE*$^{-/-}$ mice (6-8 weeks old) were given a Western type diet (TD88137, Harlan Teklad) for 20 weeks. Metformin (Sigma-Aldrich) was administered to twelve mice via the drinking water at a concentration of 250 mg/kg/day. Solutions were replaced every 2-3 days and freshly prepared based on the mice's body weight. Twelve control *ApoE*$^{-/-}$ mice were given an equal volume of plain drinking water. The animals were housed in groups of 3 per cage in a temperature- and humidity-controlled room with a 12-hour light/dark cycle. Mice had access to water and food *ad libitum*. At the end of the 20-week period, mice were fasted overnight and anesthetized with 50 mg/kg i.p. sodium pentobarbital to collect retro-orbital blood samples. Blood glucose levels were measured by the One Touch Basic glucose measurement system (One Touch). Total plasma cholesterol was analyzed by commercially available kits (Randox). The brachiocephalic artery and consecutive segments of the thoracic aorta (2 mm) were fixed in 4% formaldehyde (pH 7.4) for 24 hours and paraffin-embedded for histological analysis. In some experiments, GFP-LC3 transgenic mice (strain GFP-LC3#53, RIKEN Bio Resource Center) [32] containing a rat LC3-eGFP fusion under control of the chicken beta-actin promoter were given normal chow and treated with 250 mg/kg/day metformin or plain drinking water for 1 month. All studies were approved by the Ethical Committee of the University of Antwerp (2011-42).

HPLC-UV

PPlasma samples were deproteinized with acetonitrile (1:3 v/v) and centrifuged (1761 × g, 10 minutes) to remove precipitated proteins. Twenty µl of each sample was injected on a high performance liquid chromatography system equipped with a diode array detector (Agilent) and analyzed on a Grace RP18e – 250 x 4.6 (5µm) column (Alltech) using an isocratic mobile phase (mix 5 g Na dodecylsulfate with 1.0 ml phosphoric acid and 450 ml acetonitrile, add up to 1l with H_2O and adjust the pH till 2.6 using NaOH 1M; flow rate 1 ml/min). Metformin was detected at 236 nm and quantified using a standard curve of metformin (concentration range of 0.1 – 1µg/ml, dissolved in mobile phase). Based on a spiking experiment during which metformin standard solution was added to a non-treated mouse plasma sample prior to the sample preparation procedure, it was proven that the added metformin was fully recovered (mean recovery 105%, n=3).

Histological analysis

The plaque area (defined as the region between the lumen/intima interface and the internal elastic lamina) was measured on haematoxylin & eosin-stained sections. The acellular/anuclear area in the plaque, known as the necrotic core, was quantified in three 50 µm-spaced sections. A 3000 µm2 threshold was implemented in order to avoid counting of regions that likely do not represent substantial areas of necrosis. The cellular composition of the plaque was analyzed by immunohistochemistry using anti-α-smooth muscle cell actin (VSMCs; A2547; Sigma-Aldrich) and anti-Mac-3 (macrophages; 553322; BD Pharmingen). The endothelial coverage as well as ICAM-1 and VCAM-1 expression of ECs was measured via immunohistochemical staining using anti-CD31 (01951A, BD Pharmingen), anti-ICAM-1 (550287, BD Pharmingen) or anti-VCAM-1 (553330, BD Pharmingen) antibodies, respectively. ICAM-1 and VCAM-1 positivity was expressed as percentage of CD31 positivity. After primary antibody incubation, specimens were incubated with species appropriate horseradish peroxidase-conjugated secondary antibodies (Vector Laboratories), followed by 60 minutes of reactive ABC (Vector Laboratories). Immuno complexes were detected with 3, 3'-diaminobenzidine or 3-amino-9-ethyl-carbazole (Vector Laboratories). Collagen content was determined on Sirius red stained slides and collagen type I was quantified under polarized light. All plaque

components were expressed as percentage positivity of the total plaque area. Images were analyzed with a color image analysis system (Image Pro plus 4.1, Media Cybernetics Inc.). To investigate lipid accumulation inside the plaque, an oil red O staining was performed on Neg-50-embedded aortic tissue material. Autophago some accumulation in GFP-LC3 mice was studied by staining paraffin-embedded tissue samples with rabbit anti-LC3B (3868, clone D11; Cell Signaling Technology) as previously described [33,34].

Vascular smooth muscle cell isolation

VSMCs were isolated from mouse aorta as previously described [35]. Briefly, after excision and removal of adherent fatty tissue, the aorta was cut open starting from the diaphragm up to the aortic arch and incubated as a whole in a 100 µM calcium solution supplemented with 1.5 mg/ml papain (Sigma-Aldrich) and 0.5 mg/ml dithiothreitol (Roche Diagnostics) for 30 minutes at 37°C while being aerated by 95% O_2/5% CO_2. The entire aorta was transferred to a 100 µM calcium solution containing 2 mg/ml collagenase type II (315 IU/mg, Worthington) and incubated for 30 minutes under the same conditions. Subsequently, the aorta was flushed in 0 Ca^{2+} solution to obtain single VSMCs. After centrifugation, VSMCs were resuspended in 1:1 DMEM/F-12 medium (Life Technologies) containing 20% heat-inactivated fetal bovine serum (Sigma-Aldrich) and supplemented with 100 U/ml penicillin-100 µg/ ml streptomycin (Life Technologies) and 20 U/ml polymyxin B sulfate (Fagron). Cells were allowed to attach and grew in culture plates at 37°C in 95% O_2/5% CO_2.

Western Blot analysis

Cultured cells or homogenized aortic segments were lysed with Laemmli sample buffer (Bio-Rad). Lysates were heat-denatured for 5 minutes in boiling water and loaded on a 4-12% SDS-polyacrylamide gel. After gel electrophoresis, proteins were transferred to an Immobilon-P Transfer membrane (Millipore) according to standard procedures. Membranes were blocked in Tris-buffered saline containing 0.05% Tween 20 and 5% nonfat dry milk (Bio-Rad) for 1 hour. After blocking, membranes were probed overnight at 4°C with primary antibodies in antibody dilution buffer (Tris-buffered saline/0.05% Tween 20 containing 1% nonfat dry milk), followed by a 1 hour incubation with peroxidase-conjugated secondary antibodies (Dako) at room temperature. Antibody detection was accomplished with Super Signal West Pico or Super Signal West Femto Maximum Sensitivity Substrate (Pierce) using a Lumi-Imager (Roche Diagnostics). The following primary antibodies were used: rabbit anti-SQSTM1/p62 (P0067; Sigma-Aldrich), rabbit anti-GFP (ab6556; Abcam), mouse anti-LC3B (0231-100/LC3-5F10, clone 5F10, Nanotools), rabbit anti-AMPK (ab39644; Abcam), rabbit anti-phospho-AMPK (ab72845; Abcam), rabbit anti-ATG7 (A2856, Sigma-Aldrich), rabbit anti-GAPDH (2118; Cell Signaling Technology) and mouse anti-β-actin (AC5441; clone AC-15; Sigma-Aldrich).

siRNA transfection

HUVECs were plated in six-well plates at a density of 5×105 cells/well and allowed to adhere overnight at 37°C in M199 medium (Life Technologies), supplemented with 20% heat-inactivated FBS, 1% non-essential amino acid cell culture supplement (Life Technologies), 100 U/ml penicillin-100 µg/ml streptomycin and 150 U/ml polymyxin B. Next, cells were trypsinized, centrifuged for 10 minutes at 200 × g and resuspended in 100 µl Nucleofector Solution (Amaxa HUVEC Nucleofector Kit, Lonza). Subsequently, the cell suspension was mixed with 100 nM ON-TARGETplus *Atg7* siRNA (L-020112-00-0005, Dharmacon) or ON-TARGETplus Non-targeting siRNA (D-001810-10-05, Dharmacon) and transferred to certified cuvettes. The cuvette was placed into a Nucleofector device and the corresponding transfection program was run. After program completion, 500 µl of pre-equilibrated culture medium was added to the transfected cells and the cell suspension was gently transferred to a six-well plate. Silencing efficiency was assessed by real time RT-PCR and western blotting.

Real-time RT-PCR

Total RNA was isolated using the Absolutely RNA Miniprep Kit (Agilent Technologies) according to the manufacturer's instructions. Reverse transcription was performed at 42°C for 50 minutes with Superscript II Reverse Transcriptase (Invitrogen). Thereafter, TaqMan gene expression assays (Applied Biosystems) for ATG7, ICAM-1 and VCAM-1 were performed in duplicate on an ABI Prism 7300 sequence detector system (Applied Biosystems) in 25 µl reaction volumes containing Universal PCR Master Mix (4324018, Applied Biosystems). The parameters for PCR amplification were 95°C for 10 minutes followed by 40 cycles of 95°C for 15 seconds and 60°C for 1 minute. Relative expression of mRNA was calculated using the comparative threshold cycle method. All data were normalized for quantity of cDNA input by performing measurements on the endogenous reference gene β-actin.

Monocyte-endothelial cell adhesion

Human THP-1 cells were grown in RPMI 1640 medium containing 10% FBS and antibiotics, and labeled with 1 µ M 2',7'-Bis-(2-Carboxyethyl)-5-(and-6)-Carboxyfluorescein Acetoxymethyl Ester (BCECF-AM) for 45 minutes at 37°C. Cells were then washed twice and resuspended in Hank's Balanced Salt Solution (HBSS) at a cell density of $1x10^6$ cells/ml. To investigate monocyte adhesion, HUVECs were treated with 10 ng/ml human tumor necrosis factor-alpha (TNF-α), either alone or in the presence of metformin (10 mM). After 24 hours, $1x10^5$ BCECF-AM-labeled THP-1 cells were added and incubated at 37°C for 1 hour. Non-adherent cells were washed away with HBSS and absorbance from the remaining adhered monocytes was measured by spectrophotometry at an excitation wavelength of 485 nm and emission wavelength of 530 nm.

Statistical analysis

All data are presented as mean ± SEM and were analyzed with SPSS 23.0 software. Statistical tests are specified in the figure legends. $P < 0.05$ was considered statistically significant.

RESULTS

Metformin reduces atherogenesis and changes the cellular composition of atherosclerotic plaques

To examine whether metformin mitigates atherosclerosis, *ApoE*$^{-/-}$ mice were treated with metformin (250 mg/kg/day) via the drinking water, while feeding a Western-type diet for 20 weeks. HPLC-UV analysis showed that metformin was clearly

detectable in plasma of treated animals (1.3 ± 0.2 µg/ml), but not in plasma of untreated controls (Fig. 1). Blood glucose (control: 82 ± 6 mg/dl; metformin: 85 ± 7 mg/dl) and plasma cholesterol (control: 480 ± 42 mg/dl; metformin: 509 ± 28 mg/dl) did not significantly differ between both groups, which is consistent with earlier reports [14].

According to immunohistochemical analysis, metformin attenuated atherosclerosis and significantly reduced plaque size in the brachiocephalic artery, even though the size of the necrotic core remained unaltered (Table 1). Plaques of metformin-treated mice contained a lower amount of macrophages and an increased amount of VSMCs with a total collagen and collagen type I content that was significantly higher as compared to control mice (Table 1). Interestingly, the expression of the cell adhesion molecules ICAM-1 (intercellular adhesion molecule 1) and VCAM-1 (vascular adhesion molecule 1) was significantly decreased in metformin-treated *ApoE*$^{-/-}$ mice (Table 1). The accumulation of intracellular lipid, however, was unaffected (Table 1).

Metformin induces autophagy

Given the technical difficulties to measure autophagy *in vivo* (e.g. low levels of the well-known autophagy marker LC3) [33,34], we used GFP-LC3 transgenic mice to demonstrate induction of autophagy after oral administration of metformin. GFP-LC3 mice were treated *per os* for 1 month with 250 mg/kg/day metformin via the drinking water. Western blots of homogenized aorta tissue showed typical features of autophagy induction such as reduced levels of SQSTM1/p62 and an increased cleavage of GFP-LC3 into free GFP (Figure 2A). To confirm autophagosome formation in metformin-treated aortas, paraffin-embedded tissue samples were immuno stained for LC3B. However, even in GFP-LC3 mice, expression levels of GFP-LC3 in VSMCs were too low for immunohistochemical analysis so that stimulation of autophagosome formation by metformin was further evaluated in liver tissue. One month of metformin treatment clearly increased the formation of LC3B positive dots in the liver as compared to control treated GFP-LC3 mice (Figure 2B).

VSMCs were isolated from mouse aorta and treated *in vitro* with different concentrations of metformin (1-1000 µM). Phosphorylation of AMPK was stimulated by metformin in a concentration-dependent way, and promoted the conversion of LC3-I into LC3-II (Figure 3).

Metformin reduces monocyte adhesion to endothelial cells by down regulating expression of cell adhesion molecules

Treatment of HUVECs with TNF-α (10 ng/ml) resulted in a significant increase in mRNA expression of the cell adhesion molecules ICAM-1 and VCAM-1 (Figure 3A). Co-treatment of cells with metformin strongly inhibited TNF-α-induced expression of these cell adhesion molecules (Figure 4A) and significantly reduced the adhesion of THP-1 monocytic cells to HUVECs to a level that was comparable with THP-1 adhesion under control conditions (Figure 4B).

Down regulation of ICAM-1 and VCAM-1 by metformin depends on autophagy

To investigate whether the inhibitory effects of metformin on ICAM-1 and VCAM-1 expression is mediated by autophagy, HUVECs were transfected with *Atg7* siRNA to mimic defective autophagy. After 48 hours, ATG7 protein expression was remarkably decreased and conversion of LC3-I into LC3-II was clearly hampered, confirming defective autophagy in *Atg7* siRNA transfected HUVECs (data not shown). Under autophagy defective conditions, metformin could not inhibit TNF-α mediated stimulation of cellular adhesion molecules expression (Figure 5).

DISCUSSION

The present study demonstrates that metformin, a widely used anti-diabetic drug, impairs formation of atherosclerotic plaques in *ApoE*$^{-/-}$ mice via the induction of autophagy. Blood glucose and total plasma cholesterol levels did not change during treatment, indicating that the anti-atherogenic effects of metformin are not related to its well-known anti-diabetic and antihyperlipidemic effects. According to recent literature, autophagy is triggered during plaque formation by many pathophysiological stimuli and may exert diverse effects that restrain atherogenesis [28,36,37]. First, autophagy is a cytoprotective mechanism that protects vascular cells against cell death [28,37]. Inhibition of cell death in developing plaques prevents loss of cells that are responsible for matrix synthesis, and thus counteracts thinning of the fibrous cap, enlargement of the necrotic core as well as plaque calcification, which are all features associated with an unstable plaque phenotype. Secondly, autophagy is involved in macrophage reverse cholesterol transport and regulates the delivery of lipid droplets to lysosomes [38]. Accordingly, autophagy promotes cholesterol efflux from macrophage foam cells, thereby contributing to the regression of atherosclerotic plaques. In the present study, neither the necrotic core nor the lipid content of metformin-treated plaques changed, suggesting that inhibition of cell death or stimulation of reverse cholesterol transport as a mechanism for the anti-atherogenic effects of metformin is unlikely. Instead, we found an increased number of VSMCs and elevated collagen

Table 1: Characteristics of atherosclerotic plaques in the brachiocephalic artery of *ApoE*$^{-/-}$ mice after 20 weeks Western-type diet and treatment with metformin (250 mg/kg/day) or plain drinking water (control)

	Control	Metformin
Plaque area (x 10^3 µm ^{2})	236±30	176±18*
Necrotic core (%)	7±2	6±2
Macrophage positive area (%)	2.1±0.3	1.3±0.2*
VSMC positive area (%)	2.7±0.3	3.9±0.4*
Total collagen (%)	22±3	33±4*
Collagen type I (%)	7±1	12±2*
ICAM-1 positive ECs (%)	60±4	47±4*
VCAM-1 positive ECs (%)	20±4	10±2*
Oil red O positivity (%)	6.1±0.9	4.2±0.8

Mean ± S.E.M., n=12 per group, *$P < 0.05$; unpaired student's t-test
Abbreviations: EC: Endothelial Cell; VSMC: Vascular Smooth Muscle Cell; ICAM-1: Intercellular Adhesion Molecule 1; VCAM-1: vascular Adhesion Molecule 1

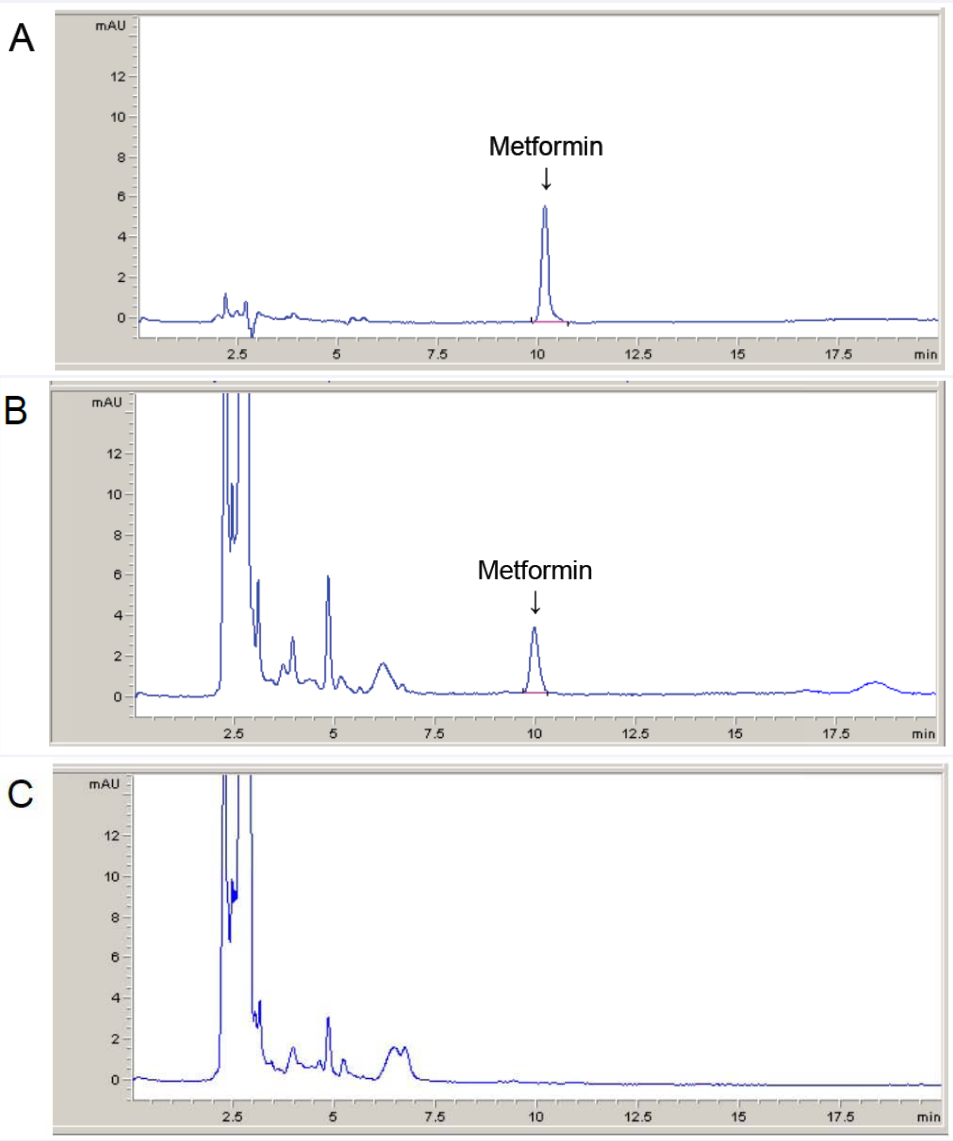

Figure 1 Metformin is detectable in plasma from metformin-treated *ApoE*$^{-/-}$ mice. HPLC chromatograms of (A) metformin standard solution, (B) plasma sample from a metformin-treated *ApoE*$^{-/-}$ mouse, and (C) plasma sample from an untreated *ApoE*$^{-/-}$ control mouse. Metformin was identified in the chromatogram of the samples based on comparison with the chromatogram of the standard solution, i.e. the retention time (about 10 min), and the similarity of the UV spectrum (not shown).

content. In line with this finding, it is important to note that autophagy, besides its role in the mechanisms mentioned above, also regulates VSMC phenotype and proliferation [28]. Induction of autophagy by platelet-derived growth factor (PDGF), for example, is associated with an enhanced potential to migrate and to proliferate, thereby promoting a synthetic VSMC phenotype [39]. Conversely, inhibition of autophagy by 3-methyladenine or spautin-1 stabilizes the contractile phenotype and reduces PDGF-induced proliferation. Similar findings were reported for the protein sonic hedgehog that induces VSMC proliferation by activation of autophagy [40].

Next to an increased number of VSMCs, we observed less macrophages in metformin-treated plaques. Along these lines, *in vitro* experiments showed that autophagy stimulation by metformin inhibits TNF-α-induced expression of the endothelial cell adhesion molecules ICAM-1 and VCAM-1, thus preventing monocyte adhesion, which is an early event in atherogenesis. Indeed, up regulation of ICAM-1 and VCAM-1 by TNF-α was blocked by metformin in autophagy -competent HUVECs, but not in autophagy-deficient cells transfected with siRNA against the essential autophagy gene *Atg7*. Importantly, disruption of basal autophagy by *Atg7* gene silencing did not affect TNFα-induced ICAM-1/VCAM-1 expression, indicating that induction of autophagy is required to prevent up regulation of ICAM-1 and VCAM-1 by TNF-α. Analogous with metformin, pretreatment of arterial ECs with resveratrol reduces TNF-α mediated expression of ICAM-1 and VCAM-1 via autophagy [41]. In addition, epigallocatechin-3-gallate that stimulates autophagosome formation in vascular ECs [42], suppresses VCAM-1 expression and consequently reduces adhesion of U937 cells in TNF-α-treated

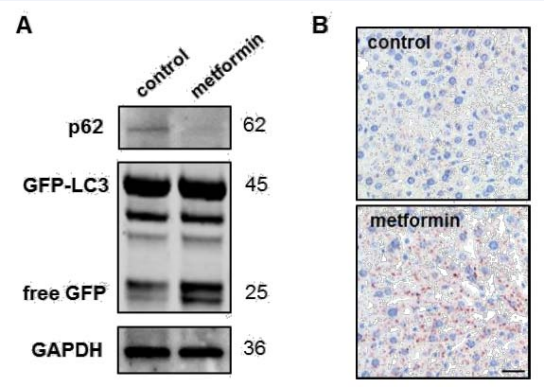

Figure 2 Metformin induces autophagy *in vivo*. GFP-LC3 mice were treated with metformin (250 mg/kg/day) for one month. (A) Western blot analysis of the autophagy-specific marker SQSTM1/p62 and cleavage of GFP-LC3 in isolated aortas of untreated (control) and metformin-treated GFP-LC3 mice. GAPDH served as a loading control. (B) LC3B-immunostained liver tissue of untreated (control) and metformin-treated GFP-LC3 mice. Scale bar = 20 μm.

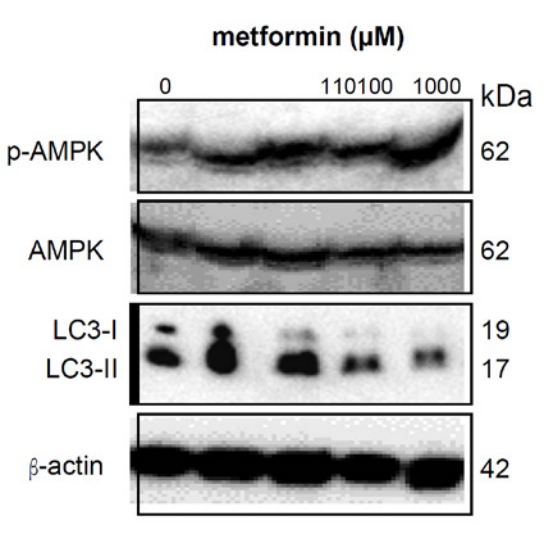

Figure 3 Metformin stimulates phosphorylation of AMPK and autophagyinduction in cultured VSMCs. Western blot analysis of AMPK, phospho-AMPK and LC3-I/-II in cultured mouse VSMCs after treatment for 24 hours with metformin (0-1000 μM). β -actin was used as loading control.

ECs [43]. Of note, metformin activates AMPK, which promotes autophagy via at least two mechanisms: mTOR inhibition and direct activation of ULK1, the mammalian homolog of yeast ATG1 that is required for initiation of autophagosome formation [44]. Moreover, stimulation of AMPK by metformin reduces cytokine-induced nuclear factor-κB (NF–κB) activation in vascular ECs [17]. NF-κB is a ubiquitous transcription factor that regulates many genes involved in inflammation [45]. Stimulation of the NF-κ B pathway by TNF-α promotes the expression of ICAM -1 and VCAM-1 and mediates leukocyte adhesion in ECs [46,47]. Interestingly, NF-κ B activation is compromised in spleens of senescence-accelerated prone 8 (SAMP8) mice that show clear signs of autophagy induction [48]. Conversely, inhibition of autophagy prevents IκB kinase degradation and rather stimulates the NF-κ B pathway [49]. These findings endorse our results and suggest that autophagy governs the expression of cell adhesion molecules in ECs, by inhibiting NF-κ B activation.

Apart from inhibition of NF-k B signaling and the prevention of monocyte adhesion, we cannot exclude that AMPK activation may result in several other anti-atherogenic effects. For example, AMPK phosphorylates and inhibits sterol regulatory element-binding protein (SREBP) activity in the liver to attenuate hyperlipidemia and atherosclerosis associated with insulin resistance [50]. Moreover, AMPK obstructs protein synthesis via inhibition of mTOR, which is associated with autophagy induction as mentioned above. Systemic administration of the mTOR inhibitor rapamycin (or derivatives thereof) in mice or rabbits strongly inhibits atherosclerotic plaque development with a substantial reduction in plaque size [51]. Because metformin and rapamycin led to similar degrees of mTOR inhibition [52], it is conceivable that metformin may act in a similar way. Adverse effects of rapamycin include dyslipidaemia and hyperglycemia, which as such are triggers of atherosclerosis. These side effects could be counteracted by co-treatment with a statin or metformin,

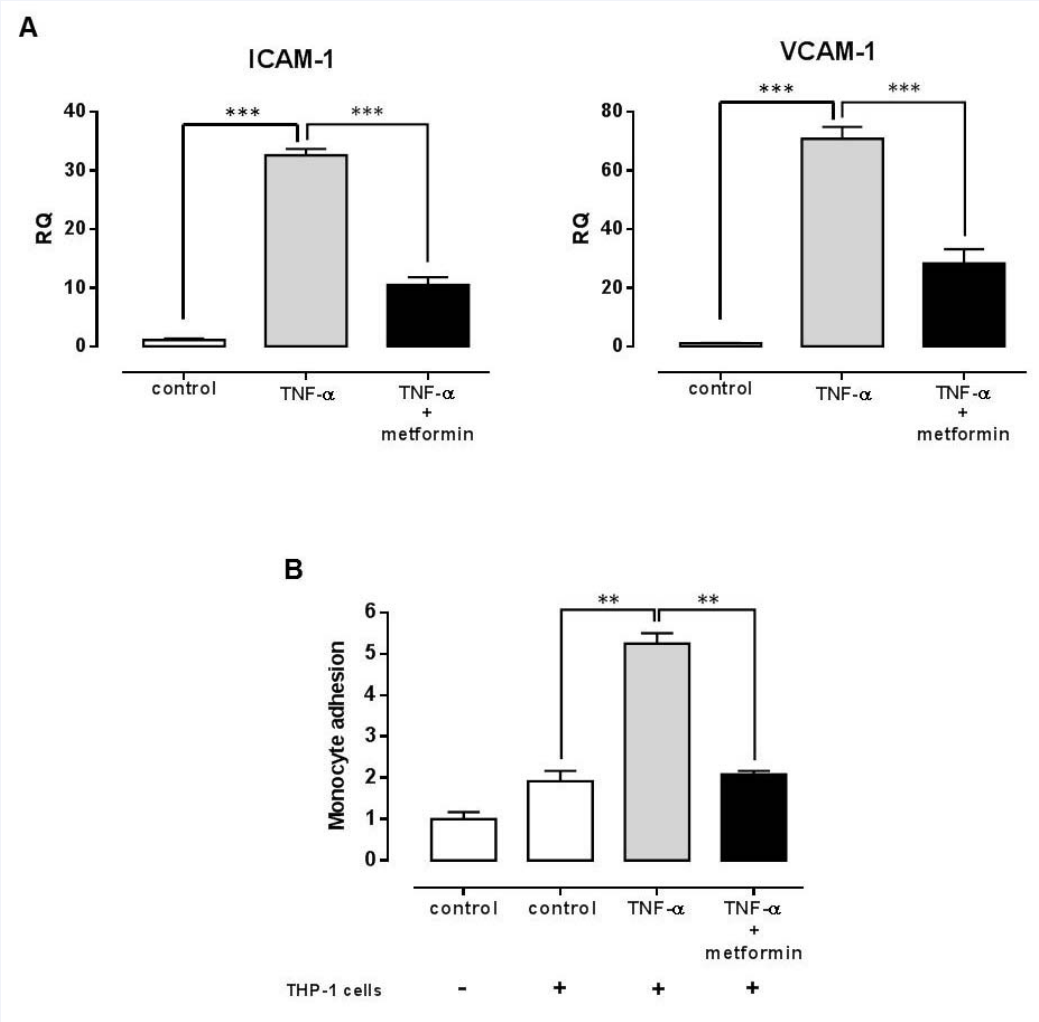

Figure 4 Metformin reduces expression of cell adhesion molecules in endothelial cells and prevents monocyte adhesion. (A) qPCR analysis of ICAM-1 and VCAM-1 expression in untreated (control) and hTNF-α (10 ng/ml) activated HUVEC cells in the absence or presence of metformin (10 mM) for 48 hours. Expression was quantified relatively (RQ) to control. (B) BCECF-AM-labeled THP-1 monocytes were added to HUVEC cells and absorbance of adhered monocytes was measured by spectrophotometry. Monocyte adhesion was relatively expressed to untreated controls in the absence of THP-1 cells. ** P<0.01, *** P<0.001 by one-way ANOVA with a Bonferroni post-hoc test (n = 4 per group for A and 3 per group for B).

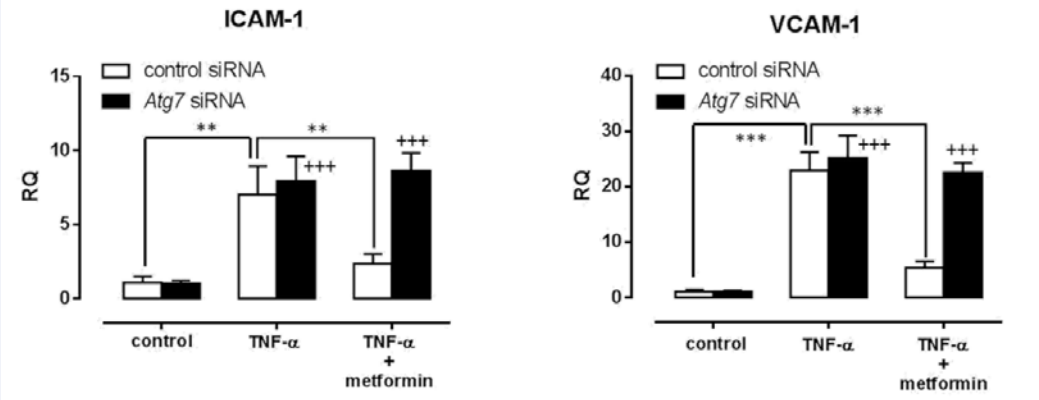

Figure 5 TNF-α mediated ICAM -1 and VCAM-1 expression by metformin is regulated by autophagy. Control siRNA and *Atg7* siRNA transfected HUVECs were activated with TNF-α (10 ng/ml) in the absence or presence of metformin (10 mM) for 48 hours. ICAM-1 and VCAM-1 expression was relatively quantified to control HUVECs. ** P < 0.01, *** P < 0.001; ^{+++}P<0.001 versus *Atg7* siRNA control (one-way ANOVA with a Bonferroni post-hoc test, n = 4 per group).

respectively, and offer an interesting therapeutic option to fully exploit the beneficial properties of mTOR inhibition in atherosclerosis [51].

CONCLUSION

The current study shows that metformin slows down atherogenesis and leads to a more stable plaque phenotype with an increased number of VSMCs, a higher collagen content and a lower amount of macrophages. Metformin indirectly prevents the accumulation of macrophages in the plaque by inhibiting the expression of the cell adhesion molecules ICAM-1 and VCAM-1 in vascular endothelial cells via induction of autophagy. Importantly, because plaque rupture is a typical feature of advanced human plaques, but rarely observed in *ApoE*$^{-/-}$ mice, it remains unclear whether metformin can prevent the life-threatening complications related to plaque rupture such as myocardial infarctions, stroke or even sudden death. Administration of metformin in a recently developed mouse model (*ApoE*$^{-/-}$*Fbn1*$^{C1039+/-}$ mice) [53] that forms advanced rupture-prone plaques may help to solve this issue. Overall, our data support previous findings showing that stimulation of autophagy exerts anti-atherogenic effects, and provide evidence for a novel mechanism in the protective action of metformin against atherosclerosis in non-diabetic subjects.

ACKNOWLEDGEMENTS

The authors acknowledge Dr Noboru Mizushima (Tokyo Medical and Dental University, Japan) for providing GFP-LC3 mice, and Rita Van den Bossche, Hermine Fret, Anne-Elise Van Hoydonck and Tania Naessens for excellent technical support. This study was funded by the University of Antwerp (BOF) and the Fund for Scientific Research (FWO)-Flanders (projects G.0074.12N and G.0443.12N). Cédéric F. Michiels is a fellow of the Agency for Innovation by Science and Technology (IWT).

REFERENCES

1. Weber C, Noels H. Atherosclerosis: current pathogenesis and therapeutic options. Nat Med. 2011; 17: 1410-1422.
2. Libby P. Mechanisms of acute coronary syndromes and their implications for therapy. N Engl J Med. 2013; 368: 2004-2013.
3. Umamahesh K, Vigneswari A, Surya Thejaswi G, Satyavani K, Viswanathan V. Incidence of cardiovascular diseases and associated risk factors among subjects with type 2 diabetes - an 11-year follow up study. Indian Heart J. 2014; 66: 5-10.
4. Shah AD, Langenberg C, Rapsomaniki E, Denaxas S, Pujades-Rodriguez M, Gale CP, et al. Type 2 diabetes and incidence of cardiovascular diseases: a cohort study in 1·9 million people. Lancet Diabetes Endocrinol. 2015; 3: 105-113.
5. Goldfine AB, Fonseca V, Shoelson SE. Therapeutic approaches to target inflammation in type 2 diabetes. Clin Chem. 2011; 57: 162-167.
6. Scheen AJ, Esser N, Paquot N. Antidiabetic agents: Potential anti-inflammatory activity beyond glucose control. Diabetes Metab. 2015; 41: 183-194.
7. Berstein LM. Metformin in obesity, cancer and aging: addressing controversies. Aging (Albany NY). 2012; 4: 320-329.
8. Goodwin PJ, Stambolic V. Obesity and insulin resistance in breast cancer-chemoprevention strategies with a focus on metformin. Breast. 2011; 3: 31-35.
9. Hadad S, Iwamoto T, Jordan L, Purdie C, Bray S, Baker L, et al. Evidence for biological effects of metformin in operable breast cancer: a pre-operative, window-of-opportunity, randomized trial. Breast Cancer Res Treat. 2011; 128: 783-794.
10. Bailey CJ. Biguanides and NIDDM. Diabetes Care. 1992; 15: 755-772.
11. Bailey CJ. Metformin: effects on micro and macrovascular complications in type 2 diabetes. Cardiovasc Drugs Ther. 2008; 22: 215-224.
12. Kooy A, de Jager J, Lehert P, Bets D, Wulffelé MG, Donker AJ, et al. Long-term effects of metformin on metabolism and microvascular and macrovascular disease in patients with type 2 diabetes mellitus. Arch Intern Med. 2009; 169: 616-625.
13. Mamputu JC, Wiernsperger NF, Renier G. Antiatherogenic properties of metformin: the experimental evidence. Diabetes Metab. 2003; 29: 71-76.
14. Forouzandeh F, Salazar G, Patrushev N, Xiong S, Hilenski L, Fei B, et al. Metformin beyond diabetes: pleiotropic benefits of metformin in attenuation of atherosclerosis. J Am Heart Assoc. 2014; 3: e001202.
15. Isoda K, Young JL, Zirlik A, MacFarlane LA, Tsuboi N, Gerdes N, et al. Metformin inhibits pro inflammatory responses and nuclear factor-kappa B in human vascular wall cells. Arterioscler Thromb Vasc Biol. 2006; 26: 611-617.
16. Huang NL, Chiang SH, Hsueh CH, Liang YJ, Chen YJ, Lai LP. Metformin inhibits TNF-alpha-induced IkappaB kinase phosphorylation, IkappaB-alpha degradation and IL-6 production in endothelial cells through PI3K-dependent AMPK phosphorylation. Int J Cardiol. 2009; 134: 169-175.
17. Hattori Y, Suzuki K, Hattori S, Kasai K. Metformin inhibits cytokine-induced nuclear factor kappa B activation via AMP-activated protein kinase activation in vascular endothelial cells. Hypertension. 2006; 47: 1183-1188.
18. Mamputu JC, Wiernsperger N, Renier G. Metformin inhibits monocyte adhesion to endothelial cells and foam cell formation. Br J Diabetes Vasc Dis. 2003; 3: 302-310.
19. Hartge MM, Unger T, Kintscher U. The endothelium and vascular inflammation in diabetes. Diab Vasc Dis Res. 2007; 4: 84-88.
20. Chen H, Li J, Yang O, Kong J, Lin G. Effect of metformin on insulin-resistant endothelial cell function. Oncol Lett. 2015; 9: 1149-1153.
21. O'Hora TR, Markos F, Wiernsperger NF, Noble MI. Metformin causes nitric oxide-mediated dilatation in a shorter time than insulin in the iliac artery of the anesthetized pig. J Cardiovasc Pharmacol. 2012; 59: 182-187.
22. Dolasik I, Sener SY, Celebi K, Aydin ZM, Korkmaz U, Canturk Z. The effect of metformin on mean platelet volume in diabetic patients. 2013; 24: 118-121.
23. Gong L, Goswami S, Giacomini KM, Altman RB, Klein TE. Metformin pathways: pharmacokinetics and pharmacodynamics. Pharmacogenet Genomics. 2012; 22: 820-827.
24. Viollet B, Guigas B, Sanz Garcia N, Leclerc J, Foretz M, Andreelli F. Cellular and molecular mechanisms of metformin: an overview. Clin Sci (Lond). 2012; 122: 253-270.
25. Mizushima N, Komatsu M. Autophagy: renovation of cells and tissues. Cell. 2011; 147: 728-741.
26. Schrijvers DM, De Meyer GR, Martinet W. Autophagy in atherosclerosis: a potential drug target for plaque stabilization. Arterioscler Thromb Vasc Biol. 2011; 31: 2787-2791.

27. Martinet W, De Meyer I, Verheye S, Schrijvers DM, Timmermans JP, De Meyer GR. Drug-induced macrophage autophagy in atherosclerosis: for better or worse? Basic Res Cardiol. 2013; 108: 321.

28. De Meyer GR, Grootaert MO, Michiels CF, Kurdi A, Schrijvers DM, Martinet W. Autophagy in vascular disease. Circ Res. 2015; 116: 468-479.

29. Liao X, Sluimer JC, Wang Y, Subramanian M, Brown K, Pattison JS, et al. Macrophage autophagy plays a protective role in advanced atherosclerosis. Cell Metab. 2012; 15: 545-553.

30. Razani B, Feng C, Coleman T, Emanuel R, Wen H, Hwang S, et al. Autophagy links inflammasomes to atherosclerotic progression. Cell Metab. 2012; 15: 534-544.

31. Grootaert MO, da Costa Martins PA, Bitsch N, Pintelon I, De Meyer GR, Martinet W, et al. Defective autophagy in vascular smooth muscle cells accelerates senescence and promotes neointima formation and atherogenesis. Autophagy; 2015; 11: 2014-2032.

32. Mizushima N, Yamamoto A, Matsui M, Yoshimori T, Ohsumi Y. In vivo analysis of autophagy in response to nutrient starvation using transgenic mice expressing a fluorescent autophagosome marker. Mol Biol Cell. 2004; 15: 1101-1111.

33. Martinet W, Schrijvers DM, Timmermans JP, Bult H, De Meyer GR. Immunohistochemical analysis of macroautophagy: recommendations and limitations. Autophagy. 2013; 9: 386-402.

34. Martinet W, Timmermans JP, De Meyer GR. Methods to assess autophagy in situ-transmission electron microscopy versus immuno histochemistry. Methods Enzymol. 2014; 543: 89-114.

35. Jackson WF, Huebner JM, Rusch NJ. Enzymatic isolation and characterization of single vascular smooth muscle cells from cremasteric arterioles. Microcirculation. 1997; 4: 35-50.

36. Martinet W, De Meyer GR. Autophagy in atherosclerosis: a cell survival and death phenomenon with therapeutic potential. Circ Res. 2009; 104: 304-317.

37. Vindis C. Autophagy: an emerging therapeutic target in vascular diseases. Br J Pharmacol. 2015; 172: 2167-2178.

38. Ouimet M, Franklin V, Mak E, Liao X, Tabas I, Marcel YL. Autophagy regulates cholesterol efflux from macrophage foam cells via lysosomal acid lipase. Cell Metab. 2011; 13: 655-667.

39. Salabei JK, Cummins TD, Singh M, Jones SP, Bhatnagar A, Hill BG. PDGF-mediated autophagy regulates vascular smooth muscle cell phenotype and resistance to oxidative stress. Biochem J. 2013; 451: 375-388.

40. Li H, Li J, Li Y, Singh P, Cao L, Xu LJ, et al. Sonic hedgehog promotes autophagy of vascular smooth muscle cells. Am J Physiol Heart Circ Physiol. 2012; 303: 1319-1331.

41. Huang FC, Kuo HC, Yu HR. Anti-inflammatory effect of resveratrol in human coronary arterial endothelial cells via autophagy: implication for the treatment of Kawasaki disease. Circulation. 2015; 131: 61.

42. Kim HS, Montana V, Jang HJ, Parpura V, Kim JA. Epigallocatechin gallate (EGCG) stimulates autophagy in vascular endothelial cells: a potential role for reducing lipid accumulation. J Biol Chem. 2013; 288: 22693-22705.

43. Yamagata K, Xie Y, Suzuki S, Tagami M. Epigallocatechin-3-gallate inhibits VCAM-1 expression and apoptosis induction associated with LC3 expressions in TNFα-stimulated human endothelial cells. Phytomedicine. 2015; 22: 431-437.

44. Kim J, Kundu M, Viollet B, Guan KL. AMPK and *mTOR* regulate autophagy through direct phosphorylation of Ulk1. Nat Cell Biol. 2011; 13: 132-141.

45. Xiao G. Autophagy and NF-kappa B: fight for fate. Cytokine Growth Factor Rev. 2007; 18: 233-243.

46. Xia YF, Liu LP, Zhong CP, Geng JG. NF-kappa B activation for constitutive expression of VCAM-1 and ICAM-1 on B lymphocytes and plasma cells. Biochem Biophys Res Commun. 2001; 289: 851-856.

47. Collins T, Read MA, Neish AS, Whitley MZ, Thanos D, Maniatis T. Transcriptional regulation of endothelial cell adhesion molecules: NF-kappa B and cytokine-inducible enhancers. FASEB J. 1995; 9: 899-909.

48. Caballero B, Vega-Naredo I, Sierra V, DeGonzalo-Calvo D, Medrano-Campillo P, Guerrero JM, et al. Autophagy up regulation and loss of NF-kappa B in oxidative stress-related immunodeficient SAMP8 mice. Mech Ageing Dev. 2009; 130: 722-730.

49. Qing G, Yan P, Xiao G. Hsp90 inhibition results in autophagy-mediated proteasome-independent degradation of Ikappa B kinase (IKK).Cell Res. 2006; 16: 895-901.

50. Li Y, Xu S, Mihaylova MM, Zheng B, Hou X, Jiang B, et al. AMPK phosphorylates and inhibits SREBP activity to attenuate hepatic steatosis and atherosclerosis in diet-induced insulin-resistant mice. Cell Metab. 2011; 13: 376-388.

51. Martinet W, De Loof H, De Meyer GR. mTOR inhibition: a promising strategy for stabilization of atherosclerotic plaques. Atherosclerosis. 2014; 233: 601-607.

52. Zakikhani M, Blouin MJ, Piura E, Pollak MN. Metformin and rapamycin have distinct effects on the AKT pathway and proliferation in breast cancer cells. Breast Cancer Res Treat. 2010; 123: 271-279.

53. Van der Donckt C, Van Herck JL, Schrijvers DM, Vanhoutte G, Verhoye M, Blockx I, et al. Elastin fragmentation in atherosclerotic mice leads to intra-plaque neovascularization, plaque rupture, myocardial infarction, stroke, and sudden death. Eur Heart J. 2015; 36: 1049-1058.

Cite this article

Michiels CF, Apers S, De Meyer GRY, Martinet W (2016) Metformin Attenuates Expression of Endothelial Cell Adhesion Molecules and Formation of Atherosclerotic Plaques via Autophagy Induction. Ann Clin Exp Metabol 1(1): 1001.